Establishment Strategy and Temporal Dynamics of *Tetrasphaera*-Enriched Microbiome for Enhanced Biological Phosphorus Removal and Recovery

Hui Wang[1,2,3], Yubo Wang[2,3], Guoqing Zhang[2], Ze Zhao[2], Feng Ju[2,3]*

[1] Environmental Science and Engineering Department, Zhejiang University, Hangzhou 310012, Zhejiang Province, China

[2] Key Laboratory of Coastal Environment and Resources of Zhejiang Province, School of Engineering, Westlake University, 18 Shilongshan Road, Hangzhou 310024, Zhejiang Province, China

[3] Institute of Advanced Technology, Westlake Institute for Advanced Study, 18 Shilongshan Road, Hangzhou 310024, China

*** Corresponding to:**

Dr. Feng Ju (Assistant Professor)

Address:

Environmental Microbiome and Biotechnology Lab (EMBLab)

Westlake University, 18 Shilongshan Road, Hangzhou 310024, China

Tel.: 571-87963205 (lab), 571-87380995 (office)

Fax: 0571-85271986

E-mail: jufeng@westlake.edu.cn

Abstract

Tetrasphaera are recently identified as among the most abundant polyphosphate accumulating organisms (PAOs) in global full-scale wastewater treatment plants (WWTPs) with enhanced biological phosphorus removal (EBPR). However, how *Tetrasphaera* PAOs are selectively enriched and functionally exploited in the context of EBPR microbiome is unclear. In this study, a *Tetrasphaera*-enriched EBPR microbiome (40% at day 113) was built using a top-down design approach featured by multi-carbon sources and low dosage of nitrification inhibitor. The microbiome showed the enhanced nutrients removal (P-removal ~85% and N-removal ~80%) and the increased P recovery (up to 23.2 times) compared with the seeding activated sludge from a local full-scale WWTP. The supply of 1 mg/L allylthiourea for 30 days gradually and largely eliminated glycogen-accumulating organisms *Ca.* Competibacter and heterotrophic *Brevundimonas*, while it promoted the co-selection of *Tetrasphaera* PAOs and *Microlunatus* PAOs, which showed a clear differentiation in niche preference, facilitating the establishment and function of EBPR microbiome. A novel putative *Tetrasphaera* PAO species EBPR-ASV0001 was identified with *T. Japonica* as its closest relative. This study provides the new knowledge for selective enrichment and functional exploitation of *Tetrasphaera* PAOs that can be further exploited to guide the future upgrading and optimizing EBPR systems in full-scale WWTPs.

Key words: Enhanced biological phosphorus removal (EBPR); Polyphosphate accumulating organisms (PAOs); *Tetrasphaera*; Microbiome; P recovery

1. Introduction

Phosphorus (P) eutrophication and P mineral resource depletion are increasingly serious global problems. Wastewater treatment plants (WWTPs) are both the sink and source for the P [1, 2]. The bioprocess known as enhanced biological phosphorus removal (EBPR) can effectively promote P removal and P recovery in WWTPs. It relies on the collection of specific microbial functional guild called polyphosphate accumulating organisms (PAOs) [3, 4]. Until now, most studies of the EBPR microbiology have focused on the *Ca.* Accumulibacter PAOs which are commonly found in full-scale WWTPs and widely enriched in lab-scale reactors using volatile fatty acids as carbon sources [4]. Because of the complex wastewater compositions and luxuriant growth conditions, full-scale WWTPs can provide diverse nutritional niches to accommodate various functional guilds [5, 6]. PAOs other than *Ca.* Accumulibacter (e.g., *Tetrasphaera* and *Dechloromonas*) are increasingly found to also play an important but previously underappreciated role in full-scale systems [4, 7, 8], which promotes the continued and follow-up efforts to explore the emerging aspects in the microbiology and ecology of the EBPR process.

Tetrasphaera PAOs have gained an increasing attention due to its prevalence in global WWTPs as both important contributors to P removal and potential reservoirs for P recovery [4]. For example, *Tetrasphaera* are found as the most abundant PAOs in 18 Danish full-scale EBPR WWTPs [7] and further revealed by Raman-FISH analysis to have a comparable or even higher P-removal contribution than *Ca.* Accumulibacter PAOs [9]. Besides, *Tetrasphaera* PAOs are implicated to metabolize various carbon sources (e.g., glucose and amino acids), which may favor their growth in WWTPs with fluctuating environmental conditions [10]. Although *Tetrasphaera* PAOs are implicated to play an important role in EBPR of full-scale WWTPs, how to selectively enrich and regulate them and how to enhance biological P removal (thus recovery) still remain elusive. Currently, *Tetrasphaera* PAOs, unlike the most intensively investigated *Ca.*

Accumulibacter, are still at an infant research stage. Our knowledge on the phylogeny, eco-physiology, and metabolism of *Tetrasphaera* PAOs and especially their capacity for wastewater P uptake and removal is limited [4, 9, 10] . The successful isolation of six *Tetrasphaera* strains partially filled the knowledge gaps, but the physiologies and metabolic characteristics of these isolates in pure culture cannot explain the interactive behaviors of *Tetrasphaera* PAOs in WWTPs [11]. Besides, the high diversity and abundance of *Tetrasphaera* PAOs in EBPR plants generally implies the existence of yet-to-be-discovered PAOs. Therefore, it is important to explore the enrichment method and microbial interactions of *Tetrasphaera* PAOs in the context of EBPR microbiome.

Until now, only several studies have reported *Tetrasphaera*-enriched microbiomes that was fed amino acids as a sole carbon source [10, 12-14], the enrichment strategy, process, and the key biotic and abiotic factors are unclear, hindering the in-depth study of ecophysiology and metabolism of *Tetrasphaera* PAOs. Noted that allylthiourea ($C_4H_8N_2S$), a specific nitrification inhibitor, is empirically supplemented to facilitate the enrichment of model PAOs (mainly *Ca*. Accumulibacter) in lab-scale EBPR reactors by suppressing nitrite and/or nitrate production to alleviate adverse competition from the denitrifying bacteria [15, 16]. Because *Tetrasphaera* PAOs possess versatile metabolism including the denitrifying capability, the effect of allylthiourea on enriching *Tetrasphaera* PAOs needs to be explored. Recently, a top-down design approach has been proposed, which uses intricately designed conditions to obtain the specific microbiome with desired functions [17]. While this new methodology framework provides an ideal theoretical guide for the *Tetrasphaera*-enriched microbiome establishment, a practical strategy is lacking and needs to be established. Also, our understanding on the microbiome dynamics and treatment performance during *Tetrasphaera*-enriched microbiome establishment process are almost blank, especially the influence of biotic and abiotic factors and the link to EBPR performance (i.e., P removal and recovery). This knowledge is the key to the reproducible establishment

and precision regulation of a *Tetrasphaera*-enriched microbiome towards improve the EBPR performance.

Given the abovementioned knowledge gaps, our study aims to i) establish and explore a top-down strategy for *Tetrasphaera*-enriched microbiome establishment and characterize its P removal and recovery potentials; ii) investigate the microbiome temporal dynamics and interaction patterns of *Tetrasphaera*-enriched microbiome establishment process; and iii) quantify the contribution of biotic and abiotic factors to the microbiome dynamics and treatment performance. Besides, the nexus between microbial composition, environmental (e.g., operational) conditions, and treatment performance of EBPR microbiome, as well as the effect of nitrification inhibitor on the enrichment of *Tetrasphaera* PAOs and EBPR performance, has also been investigated. To the best of our knowledge, this is the first proof-of-the-concept trail study to investigate the establishment approaches and mechanisms of *Tetrasphaera*-enriched microbiome from its strategy design to the potential evaluation of P recovery.

2. Materials and Methods

2.1. Bioreactor setup and operation

To enrich *Tetrasphaera* PAOs, a lab-scale sequencing batch reactor with a working volume of 10 L was established and inoculated with the activated sludge collected from a local municipal WWTP in Hangzhou, China. The WWTP employs the A/A/O process with the $AlCl_3$ coagulating sedimentation in the primary setting tank, treating 50000 m^3/d of domestic wastewater. The 8-h cycle of reactor operation consisted of four phases: 150-min anaerobic treatment, 320-min aerobic treatment, 5-min settling, and 5-min water discharge & feeding. Operation details are provided in the Supplementary Materials (Text S1).

2.2. Enrichment strategies and synthetic wastewater preparation

To selectively enrich targeted PAOs, the synthetic wastewater was prepared by adding different volume stock solutions (Table S1). Specifically, the solution A (multi-carbon sources) contained casein acid hydrolysate (CAS No. 65072-00-6, Sigma-Aldrich), glucose (CAS No.50-99-7, HuShi) and sodium acetate (CAS No.127-09-3, HuShi). The solution B (P sources) contained K_2HPO_4 and KH_2PO_4. The solution C (mineral medium) contained NH_4Cl, $MgSO_4 \cdot 7H_2O$, $CaCl_2 \cdot 2H_2O$ and trace element solution. The trace element solution was prepared according to the pervious study [15]. To investigate the effect of nitrification inhibitor on *Tetrasphaera* PAOs enrichment and EBPR function, the entire reactor operation was divided into the following four stages with different dosages of allylthiourea:

- Stage I (day 0-73): Natural enrichment phase, no allylthiourea (0 mg/L) was supplemented as nitrification inhibitor.

- Stage II (day 74-120): Reinforcement enrichment phase, the allylthiourea was supplied at 1 mg/L to enhance the *Tetrasphaera*-related PAOs enrichment by partially inhibiting nitrification activity.

- Stage III (day 121-127): Transient shock phase, the allylthiourea was added to 5 mg/L to strongly inhibit or suppress nitrification activity.

- Stage IV (day 128-170): Recovery phase, the allylthiourea concentration was adjusted back to 1 mg/L.

2.3. Batch experiments

Three batch tests were performed following experimental conditions similar to the mother reactor. Each test was seeded with the biomass collected from the EBPR reactor

on day 143 when the relative abundance of *Tetrasphaera* sequences reached 30%. The composition of synthetic wastewater was consisted with Section 2.2 but only amended with three dosage levels of allylthiourea: 0 mg/L, 1 mg/L and 5 mg/L. The pH and DO concentration were monitored using the portable multi-parameter analyzer (HQ40d, Hach, USA). Seven samples were taken at three time points of anaerobic phase (13, 45 and 135 min) and four time points of the aerobic phase (30, 90, 210 and 320 min). The sludge samples were centrifuged at 3000 rpm for 3 mins then the supernatant was collected for further physicochemical analysis.

2.4. Chemical analysis

The collected water samples were pretreated using 0.22 um Millex GP syringe driven filters to eliminate the potential solids before analysis. The PO_4^{3-}-P, TN, and NH_4^+-N were analyzed using the segmented flow analyzer (San^{++}, SKALAR, Netherlands). The TOC was assessed by the TOC-L total organic carbon analyzer (SHIMADZU, Japan). TS and VS were analyzed according to the standard methods [18]. To evaluate P recovery potential of the *Tetrasphaera*-enriched microbiome, the P weight percentage content in sludge ash was assessed and compared with the WWTP. Briefly, the sludge samples obtained from *Tetrasphaera*-enriched reactor and local WWTP (the sampling site is same with seeding sludge) were collected then adjusted to the same TS content using pure water. Samples with 50 mL volume were taken and put into a crucible for incineration (600 °C, 8h), the ash was collected and mixed using the mortar. P weight percentage content in the sludge ash was assessed by scanning electron microscope equipped with the energy dispersive spectrometer (SEM-EDS) (Hitachi, Japan). Every experiment was conducted with the triple treatments.

2.5. FISH analysis of polyphosphate accumulating organisms

Fluorescence *in situ* hybridization (FISH) analysis was performed to investigate the

spatial organization of targeted PAOs in microbiome samples, according to a pervious protocol with some modifications [19]. The detailed experiment flow and the information of FISH probe can be found in the Supplementary Materials (Text S2 and Table S2). FISH samples were observed using a laser scanning confocal microscope (Zeiss, Zeiss LSM800, Germany).

2.6. DNA extraction, PCR amplification and sequencing

Sludge samples were collected regularly at the end of the aerobic phase for DNA extraction. A total of 16 samples were collected over 170 days. DNA extraction was performed in duplicate from 1.5 ml collected reactor biomass using the Fast DNA SPIN Kit for Soil (MP Biomedicals). The duplicate DNA extracts were mixed equally for bacterial 16S rRNA gene high-throughput sequencing targeting the V1-V3 variable regions (27 F: AGAGTTTGATCCTGGCTCAG and 534 R: ATTACCGCGGCTGCTGG) [20] using Illumina's Miseq platform with a paired-end (2 × 300) sequencing strategy at the Guangdong Magigene Biotechnology Co., Ltd. China. The settings of Thermocycler (BioRad S1000, Bio-Rad Laboratory) for PCR were initial denaturation at 95°C for 2 min, 30 cycles of 95°C for 20 s, 56°C for 30 s,72°C for 60 s and final elongation at 72°C for 5 min [20].

2.7. Bioinformatics analysis

Fastp was used to control the quality of the raw data with the sliding window parameter of -W 4 -M 20. The primers were removed by using cutadapt software according to the primer information at the beginning and end of the sequence [21]. The obtained clean data was merged using QIIME2 (v. 2020.6) pipeline [22] with DADA2 algorithm[23]. The amplicon sequence variant (ASV) table was generated based on 100% sequence similarity for 16S rRNA genes. The ASVs were renamed according to the order of abundance. A specific taxonomic classifiers were trained based on

Silva_138.1_SSURef_NR99 database [24] and for taxonomic analysis.

2.8. Phylogenetic analysis

The most abundant ASVs assigned to *Tetrasphaera* was picked to construct the phylogenetic tree using MEGA X [25]. Multiple sequence alignment was conducted by MUSCLE [26] with the default parameter. The evolutionary history was inferred by the Maximum Likelihood method and Kimura 2-parameter model. Two *Nitrosomonas europaea* sequences were used as outgroup.

2.9. Statistical and network analysis

The statistical analysis including redundancy analysis (RDA), principal coordinate analysis (PCoA), and mental-test and PERMANOVA test were performed using R package vegan [27]. Co-occurrence networks were constructed using the 'Co-occurrence_network.R' script of package MbioAssy1.0 (https://github.com/emblab-westlake/MbioAssy1.0) [6, 28]. The detailed information of co-occurrence network analysis was provided in the Supplementary Materials (Text S3). The network was visualized in Gephi 0.9.2 (https://gephi.org/).

3. Results and Discussion

3.1. The establishment strategy and performance of the *Tetrasphaera*-enriched microbiome

In this study, we established a strategy including four stages to selectively enrich *Tetrasphaera* PAOs based on the top-down design approach [17]. In stage I, the multi-carbon sources (containing casein acid hydrolysate, glucose, and sodium acetate) and periodic operational condition (anaerobic/aerobic alternations) were designed as the selective tactics to conduct the initial enrichment. In stage II, 1 mg/L of allylthiourea was introduced to facilitate the enrichment by suppressing nitrification. In the following

stages (stage III and IV), a transient shock with high dosage of allylthiourea (5 mg/L) was applied to investigate the effect of allylthiourea dosage on the *Tetrasphaera*-enriched microbiome.

The treatment performance of nutrients (i.e., NH_4^+-N, TN and PO_4^{3-}-P) and organic carbon (i.e., TOC) in wastewater were followed over near six months (Fig. 1). In the stage I, the reactor showed the overall decline in P removal efficiency (average 35%) but the NH_4^+-N removal increased with the prolonged operation (the highest NH_4^+-N removal was up to 92% at day 49). With the addition of allylthiourea (stage II), the efficiency of P removal significantly increased from 27.6% (day 73) to 86.2% (day 94) and then remained stable between 83.3% and 87.4%. The NH_4^+-N removal decreased significantly during day 73 to day 90 (the lowest percentage is 3.9% at day 87) then recovered during day 105-121 (the average removal percentage is 97.6±3.0%). When the concentration of allylthiourea was purposefully increased to 5 mg/L in stage III (transient shock to suppress nitrification, Fig. 1C), the efficiency of P removal presented a slightly decreased trend (from 86.2% of day 122 to 73% of day 125), accompanying an obvious decrease and final failure in NH_4^+-N removal. With the down-regulation of allylthiourea level back to 1 mg/L on day 127 (stage IV), the efficiency of P removal was recovered to the original level (67.4% to 89.3%), and the efficiency of TN removal was stabilized at around 80% at day 148-170. Besides, the utilization and degradation of organic carbon during the 170-day operation kept stable and approximately 95% of carbon source can be absorbed and utilized (Fig. 1B).

In stage I. The noticeable increase of NH_4^+-N removal and general decrease of P removal (between day 23 and day 46, see Fig. 1A against Fig. 1C) suggested an overall negative relationship between nitrification and P removal process. Considering the high TN concentration in effluent (Fig. 1D), the nitrification production (i.e., NO_2^- and NO_3^-) may be accumulated, which could trigger the competition of denitrification for organic carbon source. Therefore, nitrification process should be controlled for promoting

PAOs enrichment and enhancing P removal. High P removal (85%) can be achieved in merely 17 days upon adding 1 mg/L allylthiourea in stage II, indicating the growth and activity of PAOs were enhanced with the regulation of nitrification inhibitor. Interestingly, the EBPR reactor can conduct the simultaneous biological N and P removal in the late phase of stage II and IV, implying the enriched microbial community may have developed the resistance to nitrification inhibitor. The effect of allylthiourea and its dosage will be further investigated in the following section 3.2.

3.2. The effect of allylthiourea on the EBPR performance

To further investigate the effect of allylthiourea on the EBPR microbiome, the batch experiments were conducted using 143-day microbiome biomass under different allylthiourea dosage (0 mg/L, 1 mg/L and 5 mg/L). The relative abundance of *Tetrasphaera* PAOs in the sampled 143-day EBPR microbiome was 30.3% (the detail information of microbiome composition and dynamics can be found in section 3.4). Besides, the corresponding removal efficiencies of PO_4^{3-}-P, TOC, NH_4^+-N and TN in mother EBPR reactor at 143 days was 91.9%, 97.9%, 92.3% and 64.4%, respectively (Fig. 1). P uptake rate with 1 mg/L allylthiourea addition was highest (0.07 mg/L·min), following by 0 and 5mg/L (0.04 and 0.05 mg/L·min, respectively) (Fig. 2A). In addition, the P removal efficiency in 5 mg/L group was 67.9%, which was lowest among three groups (Fig. 2C). The NH_4^+-N profiles of three groups were different, especially in aerobic phase. The NH_4^+-N removal was not occurring under 5 mg/L allylthiourea while a remarkable decline of NH_4^+-N concentration was observed with 0 mg/L and 1mg/L allylthiourea. For example, the NH_4^+-N concentration decreased from 24.64 mg/L to 1.48 mg/L when 1 mg/L allylthiourea was added (Fig. 2B). Besides, the dynamics of dissolved oxygen (DO) showed no visible difference in the DO concentration among the three experimental groups in anaerobic phase (< 0.2mg/L), while in the following aerobic phase the DO concentration increased to 5.21 mg/L at 53 mins when exposing

to 5 mg/L allylthiourea (Fig. 2D). In comparison, the DO concentration was 1.09 mg/L and 1.04 mg/L with an allylthiourea concentration of 0 mg/L and 1mg/L, respectively.

With the dosages of 0 and 1 mg/L allylthiourea, the enriched microbial community achieved the stable N and P removal. The result consisted with the EPBR reactor performance (described in section 3.1), indicating the community had adapted and developed resistance under the long-term selection pressure of allylthiourea in the EBPR reactor. In contrast, the high allylthiourea dosage (5 mg/L) showed a negative effect on the *Tetrasphaera*-enriched microbiome, consisting with the impact of allylthiourea addition on the nutrient removal performance afore-observed in the EBPR reactor at stage III. The increased allylthiourea dosage (5 mg/L) inhibited the nitrification process, which could cause the ammonia accumulation and disturbance for microbial community [29]. In addition, when the nitrification was completely inhibited, the production of NO_3^- and NO_2^- was decreased, which may affect the activity and function of denitrifying PAOs. To sum up, the allylthiourea can affect the *Tetrasphaera* EBPR microbiome function, EBPR microbiome can develop the resistance to low dosage allylthiourea when it was long-term supplied (i.e., 1 mg/L for 32 days in this study), contributing to the function of simultaneous N and P removal. The underlying microbiome composition, dynamics and microbial interactions will be explored later.

3.3. The FISH analysis of *Tetrasphaera*-enriched microbiome and evaluation on the P recovery potential

The *Tetrasphaera*-enriched microbiome on day 143 were visualized by FISH. The targeted *Ca.* Accumulibacter and *Tetrasphaera* PAOs were visually detected in both the seeding activated sludge flocs (A) from a full-scale WWTP and the *Tetrasphaera*-enriched microbiome (B) in our EBPR reactor (Fig. 3). Overall, *Tetrasphaera* PAOs were morphologically dominant in the EBPR microbiome, indicating that they have been successfully enriched by the top-down design approach employed. Further, the P

storage ability and recovery potential of *Tetrasphaera*-enriched microbiome were evaluated by determining the P content in the sludge ash using SEM-EDS. The P content (counted as weight percentage) in *Tetrasphaera*-enriched sludge ash and secondary sink sludge ash was 32.5% and 1.4%, respectively. Therefore, the percentage of P in *Tetrasphaera*-enriched microbiome sludge ash dramatically increased by 23.2 times compared with the normal full-scale WWTP sludge, indicating the P-storage ability of *Tetrasphaera*-enriched microbiome was largely enhanced. The strong signal intensity of Na and Mg element were detected in the *Tetrasphaera*-enriched sludge, while the Al and Si signal intensity were higher in WWTP sludge (Fig. 3C). Those results corresponded with the surface morphology of these two kinds of sludge (Fig. 3A and Fig. 3B). The WWTP sludge ash showed red color with loose structure because the influent of WWTP contained sand and the use of heavy metal coagulants. In comparison, the *Tetrasphaera*-enriched sludge ash showed white color and compact morphology, which resulted from the designed operation process and influent compositions (e.g., $MgSO_4$ and $CaCl_2$). Theoretically, the *Tetrasphaera*-enriched sludge ash is attractive to be further used for the white P recovery and promise to replace the depleting phosphate rock, in which $Ca_3(PO_4)_2$ is the main component [30]. Therefore, three essential conditions to promote the P recovery from wastewater are achieved: i) high P removal efficiency, ii) microbiome with enhanced P storage ability, and iii) P-rich ashes and compounds for further value-added P recovery. The establishment of *Tetrasphaera*-enriched microbiome holds promise for exploiting *Tetrasphaera* microbiology and EBPR biotechnology for the targeted regulation and promotion of biological P recovery in full-scale WWTPs.

3.4. The microbiome composition and dynamics during the establishment process of *Tetrasphaera*-enriched microbiome

The microbiome composition and temporal dynamics during enrichment process of *Tetrasphaera* PAOs were investigated based on high-throughput 16S rRNA gene

amplicon sequencing (Fig. 4). In general, the microbiome was dominated by *Tetrasphaera* PAOs in coexistence with *Microlunatus* PAOs and glycogen accumulating organisms (GAOs) (i.e., *Ca.* Competibacter). In seed sludge, *Tetrasphaera* PAOs, *Microlunatus* PAOs, *Brevundimonas* and *Ca.* Competibacter GAOs showed the relative abundance of 1.5%, 0.1%, 0.3% and 12.4%, respectively. With the initial establishment of EBPR microbiome, their relative abundance on day 73 was shifted to 13.5%, 2.3%, 15.1% and 3.0%, respectively. Besides, the highest relative abundance of *Tetrasphaera* PAOs was around 40% at day 113, which was 26.7 times higher than that in seed sludge (1.5%). Notably, the *Tetrasphaera* PAOs were represented by the most abundant 16S rRNA gene ASV in the EBPR microbiome (i.e., EBPR-ASV0001). Phylogenetic analysis showed that *Tetrasphaera sp.* EBPR-ASV0001 was phylogenetically different from the six previously reported isolates (Fig. 4B and Table S3). The global similarity of 16S rRNA gene sequences between EBPR-ASV0001 and *Tetrasphaera japonica* was 96.8%, indicating that EBPR-ASV0001 is most likely a denitrifying PAOs like *T. japonica*.

The abundance fluctuations of *Ca.* Competibacter GAOs, *Brevundimonas* and *Tetrasphaera* PAOs during stage I (day 0-73, Fig. 4A) consisted with the unstable biological phosphorus and nitrogen removal. In specific, *Ca.* Competibacter GAOs were negatively selected by designed operational conditions and multi-carbon sources, while the *Brevundimonas* and *Paracoccus* were markedly enriched. Besides, the decrease in the relative abundance of *Tetrasphaera* PAOs and the P removal efficiency, implying there is the negative effect caused by *Brevundimonas* and *Paracoccus*. Previous reports indicated that the occurrence of denitrification process in anaerobic phase would cause the EBPR failure because the denitrifiers would compete the organics with PAOs [16]. Especially that *Brevundimonas* and *Paracoccus* are well known not only as denitrifiers but also as the heterotrophic nitrification and aerobic denitrification (HN-AD) bacteria, which can simultaneously perform nitrification and

denitrification under the aerobic condition [31-33]. Therefore, their enrichment could not only lead competition for organics with *Tetrasphaera* PAOs but also for oxygen, especially in full-scale WWTPs where the dissolved oxygen was heterogeneous.

Interestingly in stage II, low dosage of allylthiourea (i.e., 1 mg/L) for 32 days (from day 74 to day 105) regulated the HN-AD bacteria and contributed to the simultaneous N and P removal (Fig. 1). Firstly, the following gradual increase in *Tetrasphaera* PAOs (13.0% to 37.7%) coupled to the decrease in *Brevundimonas* and *Paracoccus* (from 19.9% and 5.8% to 6.9% and 1.1%) from day 66 (stage I) to day 113 (stage II) showed that the latter genera can be correspondingly regulated to avoid the competition with former (Fig. 4A). Secondly, the remained *Brevundimonas* and *Paracoccus* have gradually established allylthiourea resistance (day 74 to 105), contributing to the subsequent recovery of nitrification activities (day 105 to 121) thus high ammonia removal (97.6±3.0%, Fig. 1C). Therefore, the strategy combining specific multi-carbon substrates, operation condition, and low allylthiourea dosage (i.e., 1 mg/L) are effective for the selective enrichment of *Tetrasphaera* PAOs, contributing to the increase in EBPR efficiency. In stage III when the transient shock of 5 mg/L allylthiourea was applied, PAOs fluctuated in their relative abundance which first decreased to 12.6% at day 147, then increased to 28.2% at day 157. We hypothesized that high allylthiourea dosage should adversely affect the proliferation and function of denitrifying PAOs that can couple nitrate and/or nitrite reduction to P uptake due to the direct suppression on nitrification. Supporting this hypothesis, ammonia removal was completely suppressed in stage III, accompanying a dramatic decline in the removal efficiency of TN and PO_4^{3-}-P to 19.5% and 58.4%, respectively (Fig. 1A). Meanwhile, high allylthiourea dosage restrained the propagation of the most abundant PAOs *Tetrasphaera* sp. EBPR-ASV0001, which showed a marked decline at day 142 (22.64%). Further genome-based study and laboratory isolation of *Tetrasphaera* sp. EBPR-ASV0001 to reveal its metabolic pathways, physiology, and application potentials in full-scale EBPR WWTP

are warranted.

3.5. The microbial co-occurrence patterns during the establishment process of *Tetrasphaera*-enriched microbiome

To predict microbial interactions in *Tetrasphaera*-enriced microbiome, microbial co-occurrence patterns over 170-day reactor operation were analyzed based on the network analysis (Fig. 5). The positive bacterial association network had 73 nodes (genera) and 204 edges (correlations, Table S4), which was topologically partitioned into six modules presumably representing discrete and interactive ecological niches over time (Fig. 5A). The topological properties of the observed network were calculated and compared with those of identically sized Erdös-Réyni random networks (Table S4). The clustering coefficient (CC) and modularity index of the observed *Tetrasphaera*-enriched co-occurrence network were 0.340 and 0.557 and higher than those of the corresponding Erdös-Réyni random networks (0.077 and 0.325), suggesting that the microbiome assembly process is non-random (or deterministic). Moreover, the network of *Tetrasphaera*-enriched microbiome showed small-world properties with a coefficient ($\sigma = \frac{\gamma}{\lambda} = \frac{C/C_{random}}{L/L_{random}}$) [34] of 3.0, showing the enrichment strategy adjusts the interior microbial interconnections and interaction patterns by creating specific niches.

To link ecological niches of co-occurring taxa to their functionality, each network node was taxonomically assigned to four functional groups (Fig. 5B), according to previous reports [7, 28, 32, 35], including organic-degrading bacteria, GAOs, PAOs, and nitrogen-removing bacteria (including AOB, NOB, denitrifiers, and HN-AD bacteria). Overall, known denitrifiers such as *Xanthobacter* in module I, *Reyranella* in module II, *Bosea* in module III, and *Defluviimonas* in module IV were broadly distributed in every major module. Likewise, organic-degrading bacteria including *Rhizobiales*, *Micavibrionales*, *Piscicoccus* and *Propioniciclava* were also distributed in module I, II, III, and IV, respectively. The wide within-module co-occurrence between organic-

degrading bacteria and denitrifiers (e.g., *Rhzobiales* and *Xanthobacter* in module I) is supported by classical presumption on their cooperative interactions such as cross-feeding, i.e., the former provides small organic molecules for the latter as carbon source. Meanwhile, the between-module interconnections show that organic-degrading bacteria may also play an important role in the establishment process of *Tetrasphaera*-enriched microbiome (e.g., by serving as a bridge for substance exchange). Especially, *Tetrasphaera* PAOs significantly co-occurred with *Xanthobacter* denitrifiers and *Aceobacteraceae* chemoorganotrophs in module I, while *Microlunatus* PAOs were positively correlated with *Paracoccus* HN-AD bacteria, *Rhodospirillaceae* heterotrophs, and *Kineosphaera* GAOs (all Spearman's $\rho > 0.60$, FDR-adjusted $P < 0.01$, Fig. 5), indicating the shared niche preference and potential cooperative relationships.

The microbial interaction and niche patterns as revealed in the co-occurrence network of *Tetrasphaera*-enriched microbiome (Fig. 5) were associated with the dynamics of removal efficiency of nutrients (A, C and D) rather than organic carbon (B, Fig. 1). First, the wide co-occurrence and prevalence of denitrifiers and organics-degrading bacteria in the same modules, together with the near-perfect TOC removal (95±1.2%) and mostly favorable TN removal (77±2.9% when no inhibition), co-implies that the chemoorganotrophic respiration and heterotrophic denitrification could be mostly active during the microbiome assembly process. Moreover, the positive correlations (Spearman's $\rho = 0.68$ and 0.69) found between *Brevundimonas* and denitrifiers (i.e., *Bosea*) generally support a prominent role of *Brevundimonas* as heterotrophic nitrifiers (as afore-discussed in Section 3.4) that may cross feed co-occurring denitrifiers with nitrification products (i.e., nitrate and nitrate). Intriguingly, despite the inhibition from low allylthiourea dosage (1 mg/L) in stage II, *Brevundimonas* and *Paracoccus* were still maintained at considerably high relative abundance (5.3±1.1% and 1.6±0.4 %). The selection and maintenance of allylthiourea-

resistant *Brevundimonas* and *Paracoccus* in stage II that can fulfill heterotrophic nitrification should have overall nutritionally benefit for the dominant denitrifying PAOs (i.e., EBPR-ASV0001) though cross-feeding, contributing to the establishment of *Tetrasphaera*-enriched microbiome (Fig. 4A) and the improvement of TN removal (from 4.5% at day 83 to 79.3% at day 108 of stage II, Fig. 1D). Likewise, a positive correlation between *Tetrasphaera* PAOs and *Xanthobacter* denitrifiers (Module I, Fig. 5A) also suggests that denitrifying phosphorus removal should have occurred in the reactor, promoting the simultaneous biological N and P removal. Prior genomic survey indicates that *Tetrasphaera* can utilize the nitrite for poly-P production [11], which could explain the above-mentioned enrichment scenarios of *Tetrasphaera* PAOs facilitated by cross-feeding partnerships with nitrate denitrifiers or ammonia oxidizers which can provide nitrate. Therefore, the intricately designed multi-carbon sources and low dosage allylthiourea create microbial niches and foster diverse cooperative interactions that regulates the microbiome composition and establishment.

3.6. The nexus between microbiome, environment, and EBPR performance

Besides microbiome dynamics and co-occurrence patterns, the role of abiotic factors (i.e., environmental condition and influent composition) and biotic factors (i.e., microbiome composition and interaction) in driving *Tetrasphaera*-enriched microbiome establishment were explored based on the RDA and PCoA analyses. The microbial communities shifted away upon reactors startup and quickly assembled with the continuous feedings of synthetic wastewater containing multi-carbon sources (S1, Fig. 6 and Fig. S1). When the nitrification inhibitor (allylthiourea) was introduced, the microbial community was significantly selected and restructured (S2, S3 and S4, Fig. 6 and Table S5). The nexus between environmental condition and microbial community was visualized with the first two RDA axes (Fig. 6A), which jointly explained 52.2% of the total microbiome variances and indicated the designed environmental parameters, especially the inhibitor (adjusted $R^2 = 0.23$, P-value < 0.01, Table S6), were among the

major drivers of the microbiome assembly process. Besides, the *Tetrasphaera* PAOs and *Microlunatus* PAOs positively correlated with the allylthiourea and PO_4^{3-}-P, indicating that *Tetrasphaera* PAOs and *Microlunatus* PAOs have the growth advantage under the selective conditions. The association analysis between microbial community and EBPR performance showed that *Tetrasphaera* PAOs, *Microlunatus* PAOs and *Saccharimonadales* positively correlated with the PO_4^{3-}-P, TN and TOC removal, meanwhile, *Brevundimonas* and *Kineosphaera* positively correlate with the NH_4^+-N removal (Fig. 6B). Consistent with RDA results, the mental-test analysis revealed that the allylthiourea significantly affected on the microbiome dynamics and PO_4^{3-}-P removal (P-value < 0.005, Table S7).

Overall, the correlations between Microbial (M) community, Environmental (E) variables, and EBPR Performance (P) (defined here as 'MEP nexus') indicated that 1 mg/L allylthiourea, as key abiotic factor, promoted the selection and proliferation of *Tetrasphaera* PAOs, *Microlunatus* PAOs and organic degrading bacteria *Saccharimonadales* and inhibited the potential competitors (e.g., *Ca.* Competibacter and some *Brevundimonas*). Meanwhile, the carbon and nutrients removal (i.e., TOC, TN and PO_4^{3-}-P) were enhanced. Notably, *Tetrasphaera* and *Microlunatus* PAOs showed no significant negative correlation in their relative abundance in the whole process (Fig. S2), and the clear differentiation in their niche preferences (Module I vs. Module II, Fig. 5A) made their co-existence feasible in *Tetrasphaera*-enriched EBPR microbiome. Besides, *Saccharimonadales*, formerly known as TM7, are reported as the key degraders of organic molecules (e.g., glucose and sugars) in aerobic sludge system [36]. Based on their temporal dynamics, *Microlunatus* PAOs and *Saccharimonadales* should be the key biotic factor which are benefited from the designed multi-carbon sources and positively contributed to building *Tetrasphaera*-enriched microbiome and enhancing the reactor performance for organics and P removal. In summary, the MEP nexus indicates that the enrichment strategy designed here have realized the selective

enrichment of *Tetrasphaera* PAOs as an outcome of synergic co-regulation from both the abiotic and biotic factors.

3.7. Final remarks and engineering significance

In this study, an enrichment strategy featured by intricately designed multi-carbon sources amended with low dosage allylthiourea was proposed and applied to build a *Tetrasphaera*-enriched EBPR microbiome. Dominated by a novel putative denitrifying *Tetrasphaera* PAO species EBPR-ASV0001 (i.e., highest relative sequence abundance of 40%), the established microbiome showed enhanced P-removal (~85%) and N-removal (~80%) and the P recovery increased 23.2 times. The addition of low-dosage allylthiourea (e.g., 1 mg/L demonstrated in this study) was showed to benefit to the establishment and regulation of the composition and dynamics of *Tetrasphaera*-enriched microbiome, and advised as a short-term bio-stimulation approach for the quick selection and enrichment of *Tetrasphaera* PAOs that strengthened biological P removal. From the MEP nexus analysis, we found that *Microlunatus* PAOs showed the differentiation in niche preference with *Tetrasphaera* PAOs by feeding on the designed multi-carbon sources, facilitated the establishment and performance improvement of *Tetrasphaera*-enriched microbiome. This finding extends our knowledges of interaction patterns of a novel putative PAO member of *Tetrasphaera*, a genus reported as the most abundant PAOs in global full-scale EBPR systems. This work outcome not only enables further in-depth study of physiology and metabolism of *Tetrasphaera* PAOs, but also provides a theoretical guidance for exploiting and optimizing EBPR applications for chemical-free and sustainable P removal and recovery in full-scale WWTPs worldwide.

Acknowledgement

This work was supported by the Key R&D Program of Zhejiang (2022C03075) and Zhejiang Provincial Natural Science Foundation of China under Grant No.

LR22D010001. We would like to thank Dr. Xiao Yang and Dr. Xiangyu Yang for the helpful discussion and technical advice. The author would like to thank Yisong Xu for her professional support on equipment procurement and lab management. We thank the Microscopy Core Facility of Westlake University for the facility support and thank technician Fang Xiao for technical assistance. We thank the Instrumentation and Service Center for Molecular Sciences and Physical Sciences at Westlake University.

References

1. Deletic, A.; Wang, H., Water Pollution Control for Sustainable Development. *Engineering* **2019,** *5*, (5), 839-840.

2. Soares, A., Wastewater treatment in 2050: Challenges ahead and future vision in a European context. *Environmental Science and Ecotechnology* **2020,** *2*, 100030.

3. Garcia Martin, H.; Ivanova, N.; Kunin, V., et al., Metagenomic analysis of two enhanced biological phosphorus removal (EBPR) sludge communities. *Nat Biotechnol* **2006,** *24*, (10), 1263-9.

4. Nielsen, P. H.; McIlroy, S. J.; Albertsen, M., et al., Re-evaluating the microbiology of the enhanced biological phosphorus removal process. *Curr Opin Biotechnol* **2019,** *57*, 111-118.

5. Ju, F.; Zhang, T., Advances in meta-omics research on activated sludge microbial community. *Microbiology China* **2019,** *46*, (2038), 14.

6. Ju, F.; Zhang, T., Bacterial assembly and temporal dynamics in activated sludge of a full-scale municipal wastewater treatment plant. *ISME J* **2015,** *9*, (3), 683-95.

7. Stokholm-Bjerregaard, M.; McIlroy, S. J.; Nierychlo, M., et al., A Critical Assessment of the Microorganisms Proposed to be Important to Enhanced Biological Phosphorus Removal in Full-Scale Wastewater Treatment Systems. *Front Microbiol* **2017,** *8*, 718.

8. Petriglieri, F.; Singleton, C.; Peces, M., et al., "Candidatus Dechloromonas phosphoritropha" and "Ca. D. phosphorivorans", novel polyphosphate accumulating organisms abundant in wastewater treatment systems. *ISME J* **2021,** *15*, (12), 3605-3614.

9. Fernando, E. Y.; McIlroy, S. J.; Nierychlo, M., et al., Resolving the individual contribution of key microbial populations to enhanced biological phosphorus removal with Raman-FISH. *ISME J* **2019,** *13*, (8), 1933-1946.

10. Liu, R.; Hao, X.; Chen, Q., et al., Research advances of Tetrasphaera in enhanced biological phosphorus removal: A review. *Water Res* **2019,** *166*, 115003.

11. Kristiansen, R.; Nguyen, H. T.; Saunders, A. M., et al., A metabolic model for members of the genus Tetrasphaera involved in enhanced biological phosphorus removal. *ISME J* **2013,** *7*, (3), 543-54.

12. Marques, R.; Ribera-Guardia, A.; Santos, J., et al., Denitrifying capabilities of Tetrasphaera and their contribution towards nitrous oxide production in enhanced biological phosphorus removal processes. *Water Res* **2018,** *137*, 262-272.

13. Marques, R.; Santos, J.; Nguyen, H., et al., Metabolism and ecological niche of Tetrasphaera and Ca. Accumulibacter in enhanced biological phosphorus removal. *Water Res* **2017,** *122*, 159-171.

14. Close, K.; Marques, R.; Carvalho, V. C. F., et al., The storage compounds associated with Tetrasphaera PAO metabolism and the relationship between diversity and P removal. *Water Res* **2021,** *204*, 117621.

15. Lu, H.; Oehmen, A.; Virdis, B., et al., Obtaining highly enriched cultures of Candidatus Accumulibacter phosphates through alternating carbon sources. *Water Res* **2006,** *40*, (20), 3838-48.

16. Guerrero, J.; Guisasola, A.; Baeza, J. A., The nature of the carbon source rules the competition between PAO and denitrifiers in systems for simultaneous biological nitrogen and phosphorus removal. *Water Res* **2011,** *45*, (16), 4793-802.

17. Lawson, C. E.; Harcombe, W. R.; Hatzenpichler, R., et al., Common principles and best practices for engineering microbiomes. *Nat Rev Microbiol* **2019,** *17*, (12), 725-741.

18. SEPA, *State Environmental Protection Administration of China (SEPA) Monitoring and Analysis Methods of Water and Wastewater*. China Environmental Science Press: Beijing, 2002.

19. Roots, P.; Wang, Y.; Rosenthal, A. F., et al., Comammox Nitrospira are the dominant ammonia oxidizers in a mainstream low dissolved oxygen nitrification reactor. *Water Res* **2019,** *157*, 396-405.

20. Albertsen, M.; Karst, S. M.; Ziegler, A. S., et al., Back to Basics--The Influence of DNA Extraction and Primer Choice on Phylogenetic Analysis of Activated Sludge Communities. *PLoS One* **2015,** *10*, (7), e0132783.

21. Martin, M., Cutadapt removes adapter sequences from high-throughput sequencing reads. *2011* **2011,** *17*, (1), 3.

22. Bolyen, E.; Rideout, J. R.; Dillon, M. R., et al., Reproducible, interactive, scalable and extensible microbiome data science using QIIME 2. *Nat Biotechnol* **2019,** *37*, (8), 852-857.

23. Callahan, B. J.; McMurdie, P. J.; Rosen, M. J., et al., DADA2: High-resolution sample inference from Illumina amplicon data. *Nat Methods* **2016,** *13*, (7), 581-3.

24. Quast, C.; Pruesse, E.; Yilmaz, P., et al., The SILVA ribosomal RNA gene database project: improved data processing and web-based tools. *Nucleic Acids Res* **2013,** *41*, (Database issue), D590-6.

25. Kumar, S.; Stecher, G.; Li, M., et al., MEGA X: Molecular Evolutionary Genetics Analysis across Computing Platforms. *Mol Biol Evol* **2018,** *35*, (6), 1547-1549.

26. Edgar, R. C., MUSCLE: multiple sequence alignment with high accuracy and high throughput. *Nucleic Acids res* **2004,** *32*, (5), 1792-1797.

27. Team, R. C., R: A language and environment for statistical computing. **2013**.

28. Ju, F.; Xia, Y.; Guo, F., et al., Taxonomic relatedness shapes bacterial assembly in activated sludge of globally distributed wastewater treatment plants. *Environ Microbiol* **2014,** *16*, (8), 2421-32.

29. Vadivelu, V. M.; Keller, J.; Yuan, Z., Effect of free ammonia on the respiration and growth processes of an enriched Nitrobacter culture. *Water Res* **2007,** *41*, (4), 826-34.

30. Yang, X.; Nohira, T., A New Concept for Producing White Phosphorus: Electrolysis of Dissolved Phosphate in Molten Chloride. *ACS Sustain. Chem. & Eng.* **2020,** *8*, (36), 13784-13792.

31. Tan, X.; Yang, Y. L.; Li, X., et al., Intensified nitrogen removal by heterotrophic nitrification aerobic

denitrification bacteria in two pilot-scale tidal flow constructed wetlands: Influence of influent C/N ratios and tidal strategies. *Bioresour Technol* **2020,** *302*, 122803.

32. Song, T.; Zhang, X.; Li, J., et al., A review of research progress of heterotrophic nitrification and aerobic denitrification microorganisms (HNADMs). *Sci Total Environ* **2021,** *801*, 149319.

33. Zhu, Z.; Yang, Y.; Fang, A., et al., Quorum sensing systems regulate heterotrophic nitrification-aerobic denitrification by changing the activity of nitrogen-cycling enzymes. *Environmental Science and Ecotechnology* **2020,** *2*, 100026.

34. Humphries, M. D.; Gurney, K., Network 'small-world-ness': a quantitative method for determining canonical network equivalence. (1932-6203 (Electronic)).

35. Tian, L.; Wang, L., Multi-omics analysis reveals structure and function of biofilm microbial communities in a pre-denitrification biofilter. *Sci Total Environ* **2021,** *757*, 143908.

36. Albertsen, M.; Hugenholtz, P.; Skarshewski, A., et al., Genome sequences of rare, uncultured bacteria obtained by differential coverage binning of multiple metagenomes. *Nat Biotechnol* **2013,** *31*, (6), 533-8.

Figure Legends

Fig. 1 The concentration (left Y axis) and removal efficiency (right Y axis) of wastewater nutrients and organic carbon during the *Tetrasphaera*-enriched microbiome establishment process. (A) Orthophosphate (PO_4^{3-}-P), (B) Total organic carbon (TOC), (C) Ammonia nitrogen (NH_4^+-N), and (D) Total nitrogen (TN).

Fig. 2 The profiles in nutrient dynamics and removal efficiency of *Tetrasphaera*-enriched microbiome with different dosages of allylthiourea. Batch experiments were set up to comparatively test the effects of 0, 1, and 5 mg/L of allylthiourea. (A) PO_4^{3-}-P dynamics; (B) NH_4^+-N dynamics. (C) Removal efficiency of PO_4^{3-}-P and NH_4^+-N. (D) DO dynamics.

Fig. 3 The fluorescence *in situ* hybridization (FISH) and elemental distribution analyses of full-scale WWTP sludge and lab-scale *Tetrasphaera*-enriched sludge. (A-B) FISH images of local WWTP sludge collected on December 2nd, 2020 (A) and *Tetrasphaera*-enriched microbiome on day 143 (B). The colors denote stained bacterial fractions in the community with all bacteria in blue, *Ca.* Accumulibater in yellow, and *Tetrasphaera* in purple. (C) Elemental distribution and weight content (%) of *Tetrasphaera*-rich sludge ash and WWTP sludge ash by scanning electron microscopy and energy dispersive X-ray spectroscopy (SEM-EDS) analysis.

Fig. 4 The microbial composition and dynamics during establishment process of *Tetrasphaera*-enriched microbiome. (A) The top 20 bacteria at genus level; (B) The dynamic and phylogenetic analysis of most abundant *Tetrasphaera*-related bacteria (EBPR-ASV0001). The evolutionary history was inferred by the Maximum Likelihood method and Kimura 2-parameter model. Two *Nitrosomonas europaea* sequences were used as outgroup. The global similarity of EBRP-ASV0001 compared with six *Tetrasphaera* isolates are provided within the brackets.

Fig. 5 Co-occurrence network of the *Tetrasphaera*-enriched microbiome based on pairwise Spearman's correlations between bacterial genera. Each connection (i.e., edge) stands for a significant Spearman's correlation coefficient > 0.6 and a *P*-value < 0.01. The size of each node is proportional to the number of connections (i.e., degree), and the thickness of edge is scaled according to the strengths of correlation between nodes. (A) Co-occurrence network colored by modularity class. (B) Co-occurrence network colored by functionality. PAOs: *Tetrasphaera*, *Microlunatus*, *Gemmatimonas*; GAOs: *Nakamurella*, *Micropruina*, *Kineosphaera*, *Kapabacteriales*, *Candidatus* Competibacter; Organic-degrading bacteria: *Micavibrionales*, *Propioniciclava*, *Piscicoccus, Rhizobiales*; Nitrogen-removing bacteria: *Xanthobacter*, *Reyranella*, *Paracoccus*, *Mesorhizobium*, *Hyphomicrobium*, *Defluviimonas*, *Brevundimonas*, *Bosea*, *Xanthobacteraceae*.

Fig. 6 Redundancy analysis (RDA) of the nexus between Microbial (M) community, Environmental (E) variables, and EBPR Performance (P). Four operational stages were defined based on the usage of nitrification inhibitor allylthiourea during the microbiome establishment process: S1: Natural enrichment phase (day 0-73) with no inhibitor; S2: Reinforced enrichment phase (day 74-120) with 1 mg/L allylthiourea as inhibitor; S3: Transient shock phase (day 121-127) with 5 mg/L allylthiourea as inhibitor); S4: Recovery phase (day 128-170) with allylthiourea dosage adjusted back to 1 mg/L. The dash arrow lines denote two adjacent sampling time points in the first 73 days after reactor startup.

Figures

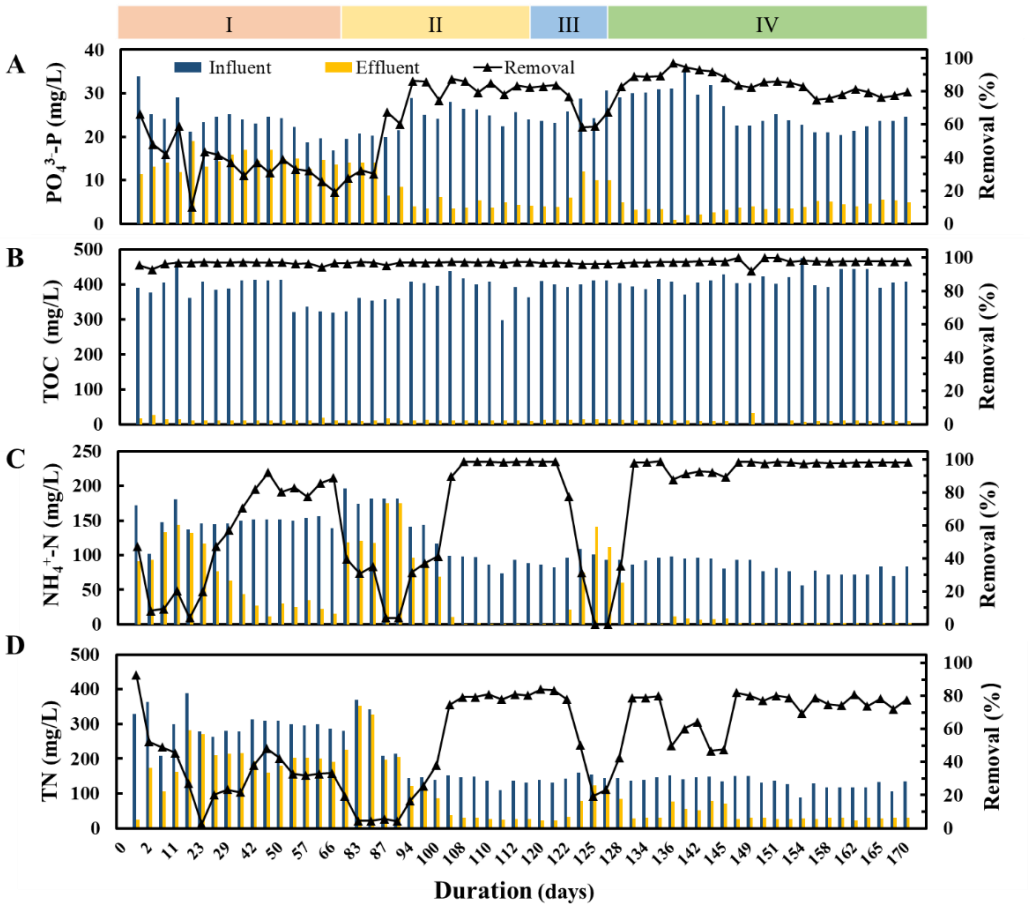

Fig. 1 The concentration (left Y axis) and removal efficiency (right Y axis) of wastewater nutrients and organic carbon during the *Tetrasphaera*-enriched microbiome establishment process. (A) Orthophosphate (PO_4^{3-}-P), (B) Total organic carbon (TOC), (C) Ammonia nitrogen (NH_4^+-N), and (D) Total nitrogen (TN).

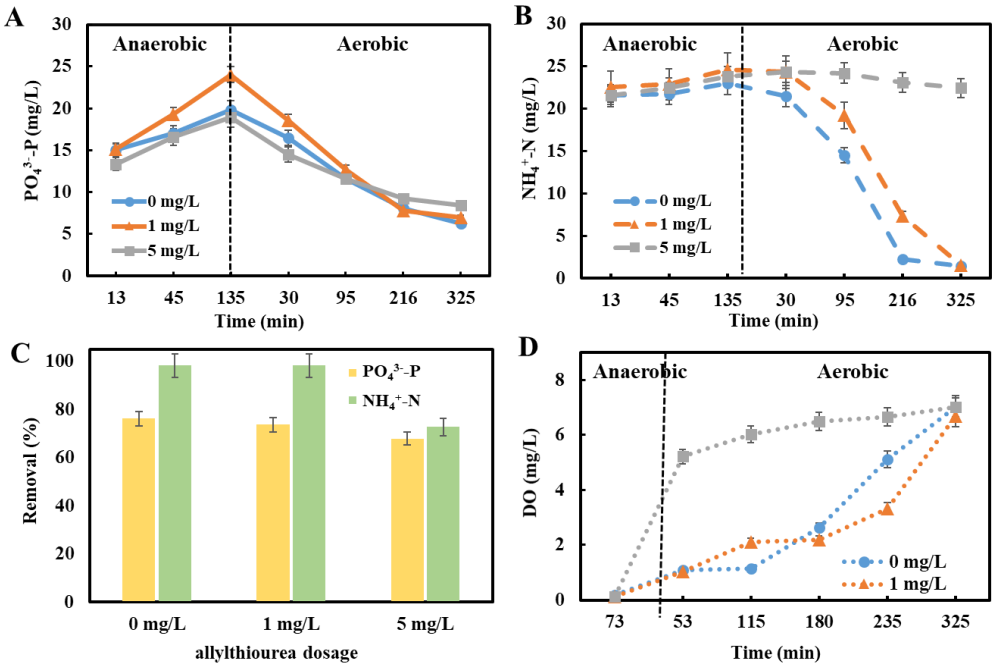

Fig. 2 The profiles in nutrient dynamics and removal efficiency of *Tetrasphaera*-enriched microbiome with different dosages of allylthiourea. Batch experiments were set up to comparatively test the effects of 0, 1, and 5 mg/L of allylthiourea. (A) PO_4^{3-}-P dynamics; (B) NH_4^+-N dynamics. (C) Removal efficiency of PO_4^{3-}-P and NH_4^+-N. (D) DO dynamics.

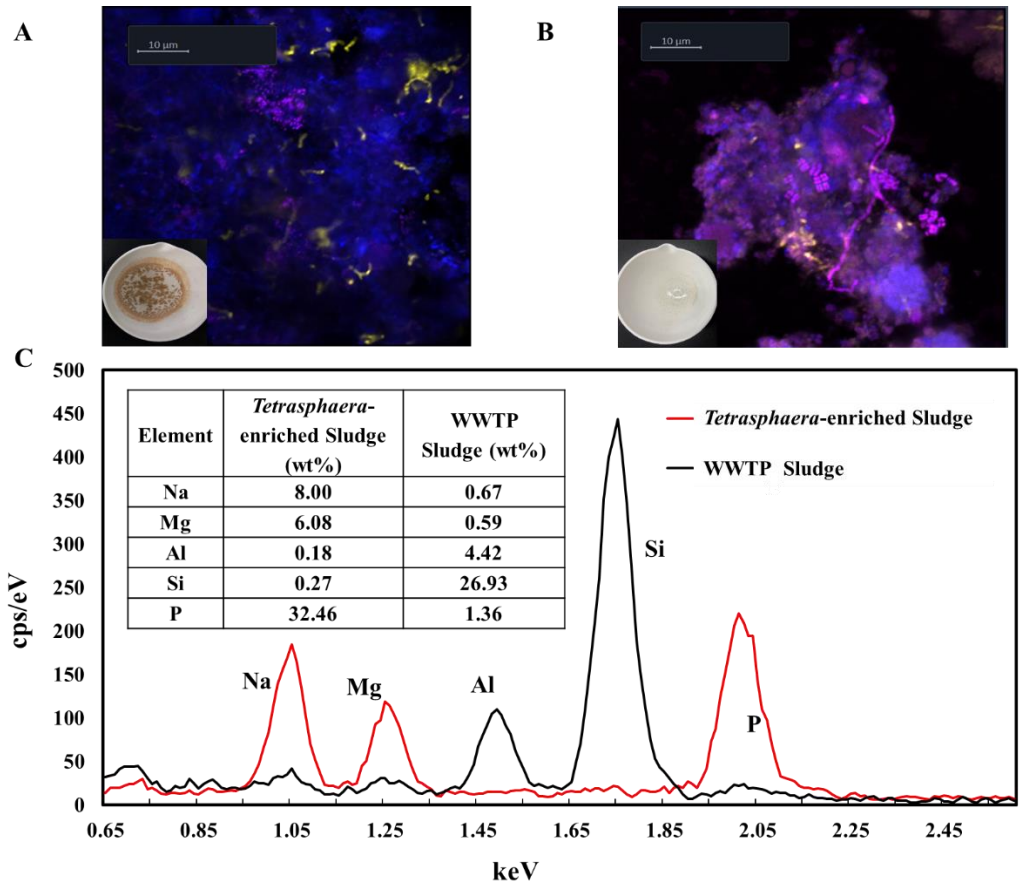

Element	*Tetrasphaera*-enriched Sludge (wt%)	WWTP Sludge (wt%)
Na	8.00	0.67
Mg	6.08	0.59
Al	0.18	4.42
Si	0.27	26.93
P	32.46	1.36

Fig. 3 The fluorescence *in situ* hybridization (FISH) and elemental distribution analyses of full-scale WWTP sludge and lab-scale *Tetrasphaera*-enriched sludge. (A-B) FISH images of local WWTP sludge collected on December 2nd, 2020 (A) and *Tetrasphaera*-enriched microbiome on day 143 (B). The colors denote stained bacterial fractions in the community with all bacteria in blue, *Ca.* Accumulibater in yellow, and *Tetrasphaera* in purple. (C) Elemental distribution and weight content (%) of *Tetrasphaera*-rich sludge ash and WWTP sludge ash by scanning electron microscopy and energy dispersive X-ray spectroscopy (SEM-EDS) analysis.

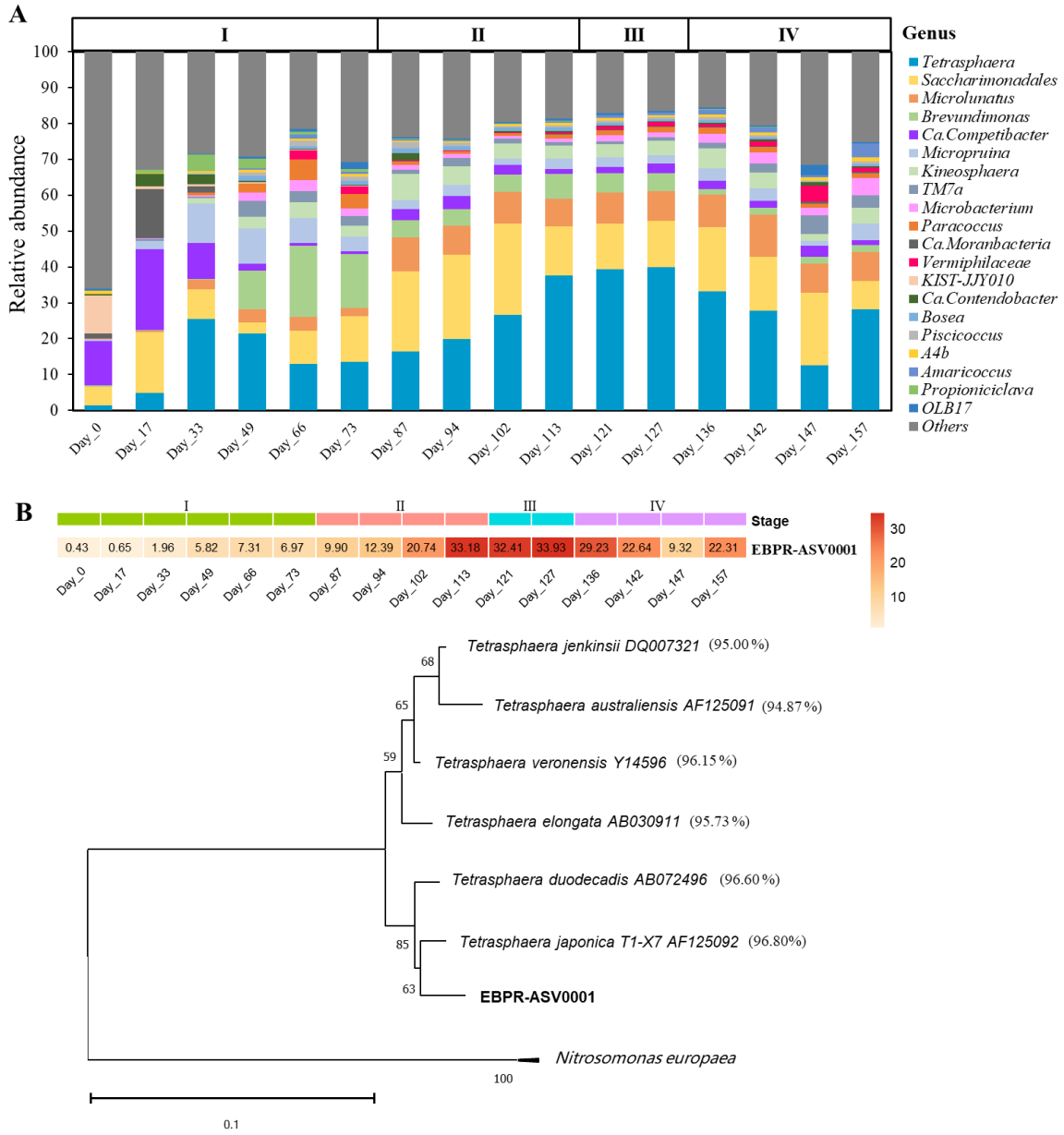

Fig. 4 The microbial composition and dynamics during establishment process of *Tetrasphaera*-enriched microbiome. (A) The top 20 bacteria at genus level; (B) The dynamic and phylogenetic analysis of most abundant *Tetrasphaera*-related bacteria (EBPR-ASV0001). The evolutionary history was inferred by the Maximum Likelihood method and Kimura 2-parameter model. Two *Nitrosomonas europaea* sequences were used as outgroup. The global similarity of EBRP-ASV0001 compared with six *Tetrasphaera* isolates are provided within the brackets.

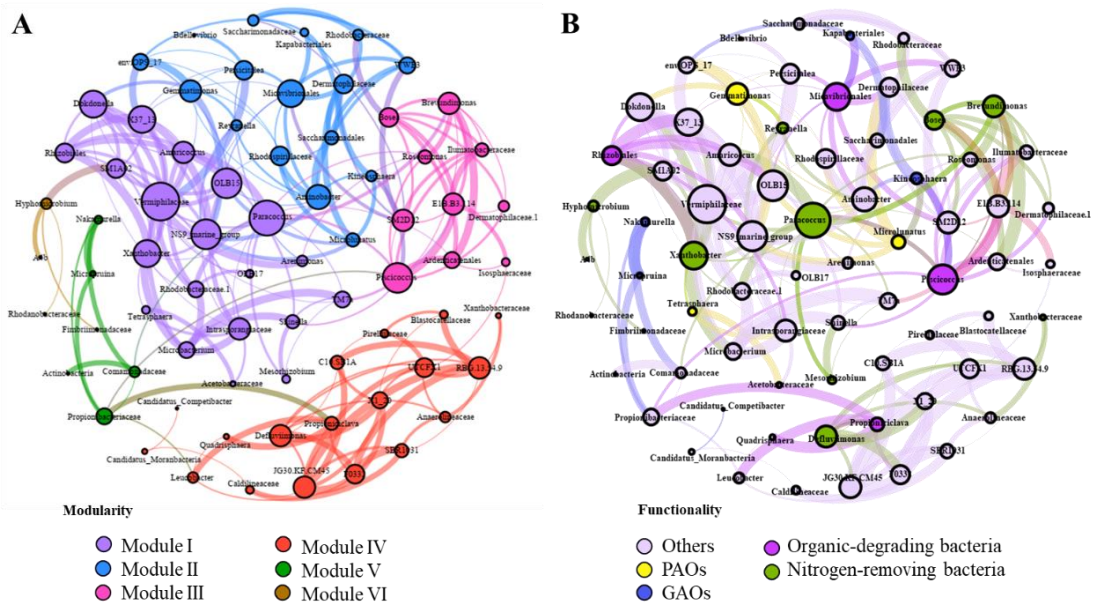

Fig. 5 Co-occurrence network of the *Tetrasphaera*-enriched microbiome based on pairwise Spearman's correlations between bacterial genera. Each connection (i.e., edge) stands for a significant Spearman's correlation coefficient > 0.6 and a *P*-value < 0.01. The size of each node is proportional to the number of connections (i.e., degree), and the thickness of edge is scaled according to the strengths of correlation between nodes. (A) Co-occurrence network colored by modularity class. (B) Co-occurrence network colored by functionality. PAOs: *Tetrasphaera*, *Microlunatus*, *Gemmatimonas*; GAOs: *Nakamurella*, *Micropruina*, *Kineosphaera*, *Kapabacteriales*, *Candidatus* Competibacter; Organic-degrading bacteria: *Micavibrionales*, *Propioniciclava*, *Piscicoccus, Rhizobiales*; Nitrogen-removing bacteria: *Xanthobacter*, *Reyranella*, *Paracoccus*, *Mesorhizobium*, *Hyphomicrobium*, *Defluviimonas*, *Brevundimonas*, *Bosea*, *Xanthobacteraceae*.

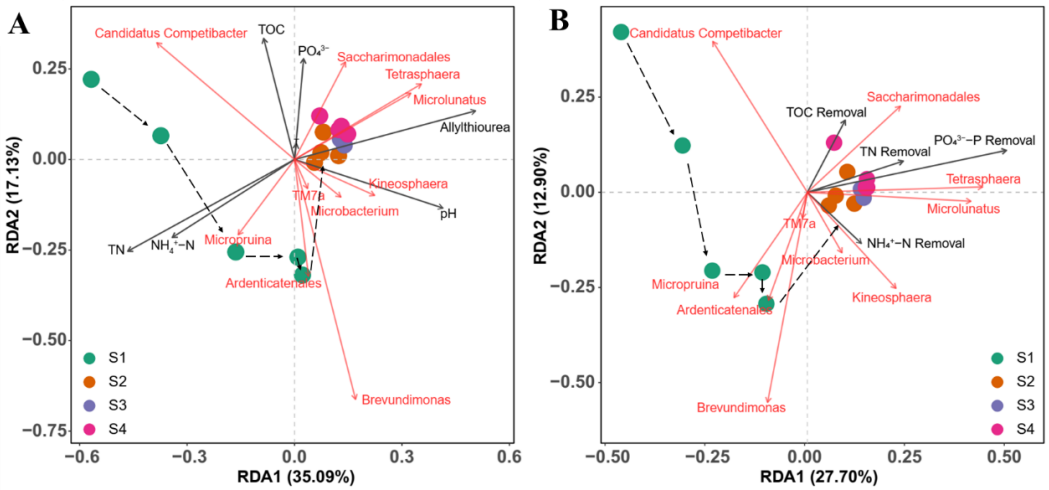

Fig. 6 Redundancy analysis (RDA) of the nexus between Microbial (M) community, Environmental (E) variables, and EBPR Performance (P). Four operational stages were defined based on the usage of nitrification inhibitor allylthiourea during the microbiome establishment process: S1: Natural enrichment phase (day 0-73) with no inhibitor; S2: Reinforced enrichment phase (day 74-120) with 1 mg/L allylthiourea as inhibitor; S3: Transient shock phase (day 121-127) with 5 mg/L allylthiourea as inhibitor); S4: Recovery phase (day 128-170) with allylthiourea dosage adjusted back to 1 mg/L. The dash arrow lines denote two adjacent sampling time points in the first 73 days after reactor startup.